Citation:
House, C, Hancock, N, Moller, A, Cromer, B, Fedorov, V, Bowtell, D, Parker, M and Polekhina, G 2006, 'Elucidation of the substrate binding site of Siah ubiquitin ligase', Structure, vol. 14, no. 4, pp. 695-701.

Elucidation of the substrate binding site of Siah ubiquitin ligase

Colin M House[1], Nancy C Hancock[2], Andreas Möller[1], Brett A Cromer[2], Victor Fedorov[2,3], David D L Bowtell[1], Michael W Parker[2] & Galina Polekhina[2]

[1]Ian Potter Foundation Centre for Cancer Genomics and Predictive Medicine, Peter MacCallum Cancer Centre, Locked Bag 1, A'Beckett St., Melbourne, Victoria 8006, Australia.

[2]Biota Structural Biology Laboratory, St. Vincent's Institute of Medical Research, 41 Victoria Parade, Fitzroy, Victoria 3065, Australia.

[3]Current address: Department of Chemistry, Gottwald Science Center, University of Richmond, VA 23173, USA.

Correspondence should be addressed to D.D.L.B. (david.bowtell@petermac.org) or M.W.P. (mparker@svi.edu.au).

Summary

The Siah family of RING proteins function as ubiquitin ligase components, contributing to the degradation of multiple targets involved in cell growth, differentiation, angiogenesis, oncogenesis and inflammation. Previously, a binding motif (degron) has been recognized in many of the Siah degradation targets, suggesting that Siah itself may facilitate substrate recognition for a subset of its targets. We report the crystal structure of the Siah in complex with a peptide containing the degron motif. Binding is within a groove formed in part by the zinc fingers and the first two β-strands of the TRAF-C domain of Siah. We show that residues previously described to facilitate binding to Siah interact with the protein and mutagenesis of Siah at sites of interaction abrogate both *in vitro* binding to and *in vivo* degradation of known Siah targets.

Protein poly-ubiquitylation functions as a signal for protein degradation by the 26S proteasome. One mechanism of protein ubiquitylation involves three steps – activation of ubiquitin by an E1 enzyme, transfer to a carrier protein (E2) and ligation to the target in the presence of a ligase protein/complex (E3). The E2 and more especially the E3 proteins confer specificity for targeting ubiquitylation[1].

Drosophila SINA (Seven in Absentia) and mammalian Siah (Seven in Absentia Homologue) are RING-containing proteins that function in protein degradation as parts of ubiquitin ligase (E3) components. In *Drosophila*, SINA has been shown to co-operate with Phyllopod (PHYL), Ebi and UBCD1 to facilitate the ubiquitylation and degradation of the transcriptional co-repressor Tramtrack 88 (TTK88)[2-5]. In mammalian cells, a similar complex comprising Siah1, Siah-interacting protein (SIP), and the F-box protein Ebi bind to adenomatous polyposis coli (pAPC) to facilitate the ubiquitylation and degradation of β-catenin via a p53-dependent mechanism[6]. As well, Siah has been reported to bind directly to many proteins that are subsequently degraded, suggestive of a simpler E3 complex[7]. Structurally, little is known about the E3 complexes formed with this family of proteins. It has been suggested that they form a novel complex similar to, but distinct from, the generic RING-containing E3 complexes characterized by the anaphase-promoting complex (APC) and the Skp1/Cul1/F-box protein (SCF) ligases. The Siah protein's dimeric nature alone suggests a variant complex, since none of the described complexes contain dimeric RING proteins.

Siah has recently received a great deal of attention because of its role in certain disease processes. For example, Siah regulates hypoxia-inducible factor-1alpha protein levels, itself a central regulator of the cellular response to hypoxia by hypoxia-induced interaction and

degradation of PHD prolyl hydroxylases[8]. Siah also interacts with synphilin-1 and α-synuclein and thus may play a role in Parkinson's Lewy body formation[9].

Siah is a dimeric protein consisting of an N-terminal RING domain followed by two novel zinc finger motifs and a C-terminal substrate-binding domain (SBD). We have previously described the crystal structure of the murine Siah1a (missing the RING domain) to 2.6 Å resolution[10]. The structure revealed that Siah is a dimeric protein with each SBD adopting an eight-stranded β-sandwich fold. Each SBD is extended at the N-terminus by a tandem pair of zinc fingers. Analysis of the surface of the molecule suggested a number of regions that might interact with protein ligands. The dimer has two deep clefts located adjacent to the N-terminal zinc fingers of each monomer and a larger but shallower groove centred about the dimer interface. We hypothesised that the clefts might be filled by the RING domains that are N-terminal to the zinc fingers in the intact Siah molecule. The large shallow groove (~ 30 Å wide), constructed from a curved anti-parallel β-sheet that straddles the dimer interface, was considered as an alternative location for a protein-protein interaction region. Reed and Ely[11] noted that the deep clefts have an overall electropositive potential whereas the shallow groove was strikingly electronegative. Mutagenesis of carboxylate residues (Glu161, Asp162, Glu226, Glu237) in the shallow groove of Siah resulting in loss of binding to the Siah-interacting protein, SIP, whereas mutations of basic residues in the deep clefts (Arg124, Arg214, Arg215, Arg231, Arg232) had no effect[12]. Interestingly, the binding of another Siah ligand, BAG1, was unaffected by mutations in either groove or cleft[12]. More recently we reported that many Siah-binding proteins contain a common binding motif that may act as a degradation signal or 'degron'[13]. However, attempts to computationally dock the consensus motif onto the Siah structure did not reveal the binding site for the degron (unpublished results).

Here we report the crystal structure of the Siah bound to a degron motif-containing peptide that reveals a binding site for Siah-interacting proteins. This site is distinct from those previously hypothesised as protein interaction sites. We further show that mutation of Siah residues seen to interact with the degron abrogate binding to multiple partners, as well as inhibiting cellular proteasomal degradation of such proteins in co-transfection experiments.

RESULTS

Structure of the Siah bound to PHYL (107-130) peptide

We have determined the crystal structure of Siah (residues 92 to 282) in complex with the synthetic peptide encompassing residues 107-130 of Phyllopod (PHYL) (**Fig. 1**), which includes the earlier identified common degron motif[13]. The structure of the complex was determined by molecular replacement using the previously published Siah (92-282) structure composed of two zinc fingers and the SBD[10] (see Methods for a full description). There are four copies (two dimers AB and CD) of the Siah:PHYL complex in the asymmetric unit. The SBDs of the two dimers superimpose closely with an average root-mean-square deviation (rmsd) on Cα's of 0.3 Å. Monomers A and C (SBD and fingers) superimpose with a rmsd on Cα's of 0.45 Å. However, the rmsd on superposition of monomers B and D is much higher (0.9 Å) due to a shift of the N-terminal zinc finger domain with respect to each other.

Superposition of the complex structure on the published Siah structure reveals no significant conformational changes beyond movements of the zinc finger domains and some loops. Superposition of the SBDs (excluding the loop 195-204 of each monomer which have fairly divergent conformations in the complex structure – see below) yields an average rmsd on Cα's of 0.7 Å. The zinc finger domains appear more ordered in the complex structure, likely due to crystal lattice effects. If the SBDs of the complex and uncomplexed structures

are superimposed a large shift in the position of the first zinc finger is observed (5 or 9 Å depending on which monomer is compared) and a small shift (~ 1.5 to 2 Å) occurs in the position of the second zinc finger domain. A loop between residues 172 and 177 adopts a different conformation in the complex compared to the uncomplexed structure due to interaction with the PHYL peptide. However, the conformation of this loop in all four monomers of the complex structure is very similar. The loop at the tip of the dimer interface (residues 195-204) adopts a similar conformation in all 4 monomers of Siah but a different conformation to that of the uncomplexed structure due to the absence of a zinc ion. In the uncomplexed structure a zinc atom was located at the tip of the dimer interface and coordinated by Asp200, His202 from monomer and His202 of another monomer and His150 of symmetry-related molecule. We had previously suggested that this zinc site was unlikely to be physiologically relevant[10].

The structure of the complex reveals the PHYL peptide-binding site located in a shallow surface groove formed by the beta-sandwich of the Siah SBD and β0 strand making up the connection between the second zinc finger domain and SBD (**Fig. 1**). Thus, there are two PHYL peptide binding sites on the Siah dimer separated by 45 Å. The peptide spans a length of 30 Å across the surface of the protein, from the concave surface formed by the anti-parallel beta-sheet at one end of the dimer to the tip at the other end of the dimer (**Fig. 1**).

Peptide-protein interactions further define the degron motif

Good electron density is observed for PHYL residues 114 to 124. The PHYL peptide adopts an extended conformation, packing against the β1 and β2 strands of the beta-sandwich of the Siah SBD (**Figs. 1a,b**). The peptide makes several parallel beta-sheet interactions between its main chain and the main chain atoms of the β1-strand in Siah: the main chain carbonyl of

Pro116 (PHYL) interacts with the main chain amide of Val164, the main chain amide and carbonyl moieties of Ala118 (PHYL) interact with the main chain carbonyl of Val164 and the amide of Leu166, the main chain amide and carbonyl moieties of Val120 (PHYL) interact with the main chain carbonyl moiety of Leu166 and main chain amide of Thr168. The peptide is also involved in anti-parallel beta-sheet interactions with the β2-strand of Siah: the main chain amide and carbonyl moieties of Thr123 (PHYL) interact with the main chain carbonyl and amide moieties of Asp177 (β2, Siah).

There are a number of contacts involving side-chains (**Figs. 1b,c**) that are identical in all four binding sites observed in the asymmetric unit. Arg115 (PHYL) is in hydrogen bonding distance with Asp162 and Asn276. These residues are located in the concave surface formed by the anti-parallel beta-sheet that straddles across the Siah dimer. Val117 (PHYL) is in van der Waals contact with Val164 (β1, Siah) and Leu166 (β1, Siah). Ala118 (PHYL) is packed against Met180 (β2, Siah) and Leu158 (β0, Siah). The distances between the CB atom of Ala118 and CE, SD atoms of Met180 and CD2 atom of Leu158 are 3.4 Å, 3.7 Å and 4.1 Å respectively. Val120 (PHYL) is in van der Waals contact with Phe165 (β1, Siah), Met180 (β2, Siah) and Trp178 (β2, Siah). The distances between the CG2 atom of Val120 and the CD2 atom of Phe165, the CB atom of Val120 and CE2 atom of Phe165, the CG1 atom of Val120 and CB atom of Trp178, the CG2 atom of Val120 and the CB atom of Met180 are 4.2 Å, 4.5 Å, 4.2 Å and 3.8 Å respectively. The binding pockets for Ala118 and Val120 are too small to accommodate larger side chains. Pro122 (PHYL) packs against Trp178 (β2, Siah), a residue that is strictly conserved in the Siah/Sina family of proteins.

There are a number of local changes observed in the Siah structure upon PHYL binding. The β0 strand shifts by about 1.5 Å away from the core of SBD. The side chain conformation of Phe165 is altered as manifested by a change in its chi2 angle from about 50˚

to 180˚. This in turn causes the side chain of Leu191 to swing out of the way. The side chain orientation of Leu158 is also altered to accommodate Ala118 of the PHYL peptide. The same changes are seen in all 4 monomers in the asymmetric unit.

Mutation of Siah residues that interact with PHYL (107-130) abrogates binding to PHYL *in vitro*

We used the crystal structure of the complex as a guide for mutagenesis studies in order to determine the relative importance of various interacting residues of Siah with its degron target (PHYL). We mutated Met180 to Lys to disturb the hydrophobic pocket harbouring Ala118 and Val120 of PHYL in the complex (**Fig. 1c**). We also targeted residues located in β0 (Thr156 and Leu158) and β1 (Leu166, Thr168), as well as the residue Ala175 from the loop 172-177 to probe the role of PHYL residues 125 to 130 in the binding (**Fig. 1b**). Leu158Lys, Leu158Asp, Thr168Arg, Leu166Lys, Ala175Glu, as well as the double mutations Thr156Glu/Leu158Asp and Leu166Lys/Thr168Arg, were prepared.

The effects of the mutations were tested in *in vitro* pull down assays as described in the Methods. The results are presented in **Figure 3**. Met180Lys almost completely abolishes binding of the target by Siah, underlying the importance of the hydrophobic interaction observed in the crystal structure and suggesting that it is a key recognition/specificity point. The mutations in strand β0 had more pronounced effects than the mutations in β1. The side chains of the residues from strand β0 point into the PHYL binding groove of Siah. Ala175Glu has slightly increased PHYL binding, which may be due to potential additional hydrogen bonding contacts provided by the Glu side chain towards PHYL, particularly considering that the PHYL residue 125 that interacts with Siah at that position is an arginine residue.

Siah binding mutants fail to facilitate degradation of substrates

To examine whether the identified binding site is also responsible for the binding induced degradation of Siah targets in mammalian cells, we examined the Siah substrate TIEG-1. The transcriptional repressor, TIEG-1, is a mammalian degradation target for Siah[14] that also possesses the consensus degron motif[13]. To investigate the relevance of the peptide-binding site to substrate protein degradation, co-transfection experiments were performed in mammalian HEK293T cells. Siah was shown to increase the rate of degradation of TIEG-1 when co-transfected (**Fig. 3**). Degradation was shown to be proteasome-dependent by the addition of the proteasome inhibitor MG132 (**Fig. 3b**). When mutant Siah was introduced in these experiments, TIEG-1 degradation was affected to varying degrees mirroring the pull down assay results (cf. **Figs. 2** and **3a**). In particular, mutations in β1-strand of Siah involving residues Leu166 and Thr168 that only partly disrupted PHYL binding (**Fig. 2**) did not rescue TIEG-1 degradation (**Fig. 3a**). Siah mutants at Met180 and Leu158, which bound PHYL peptide poorly (**Fig. 2**), failed to degrade TIEG-1 (**Fig. 3a**). The mutation of Ala175 to glutamate apparently promoted the binding of PHYL to Siah (see above and **Fig. 2**), and this mutant was effective in promoting TIEG-1 degradation. To further substantiate that TIEG-1 binds Siah via the degron motif, we mutated the important Val and Pro within TIEG-1 and showed that it was no longer degraded in the presence of co-transfected Siah (**Fig. 3c**).

DISCUSSION

The structure of the complex between Siah (residues 92 to 282) and PHYL (residues 107-130) reveals that the degron recognition site is located in a shallow surface groove formed by the beta-sandwich of the Siah SBD and a β-strand that connects the second zinc finger domain to SBD. This site has not previously been identified as a possible protein interaction site. There

are two PHYL peptide-binding sites per dimer with each peptide spanning a length of 30 Å across the surface of the protein (**Fig. 1**). The structure provides a molecular basis for understanding the importance of the previously published degron motif, Pro-X-Ala-X-Val-X-Pro[13]. Pro116, Ala118, Val120 and Pro122 are all in direct contact with Siah in the complex structure. Ala118 and Val120 embed their side chains into the hydrophobic core of the beta-sandwich where the binding pockets are too small to accommodate larger side chains. Pro116 and Pro122 ensure the extended conformation of the motif for optimal presentation of the main chain carbonyls and amides of PHYL to the backbone atoms of the β strands of Siah. Pro122 also packs against the conserved Siah residue Trp178.

In the Siah:PHYL complex crystal structure we only observe electron density corresponding to 114-124 of PHYL even though the peptide used in the crystallization included residues 107 to 130. Thus residues 108-113 and 125-130 are flexible and could not be modelled. Non-consensus residues that do interact with Siah include Arg115 and Thr123. Arg115 interacts with an acidic patch on Siah's concave surface involving residue Asp162 that was previously implicated in substrate recognition[12] and Asn276. Modelling suggests that Arg111 or Lys113 could form a salt bridge to either Glu161 or Glu226 (although the peptides from the two binding sites could clash in this case). Arg125 on the C-terminal end of PHYL could form a salt bridge with Glu194 (a strictly conserved residue in Siah) or to Glu197. However, the latter is unlikely to be a significant interaction as it would be expected to have been disrupted by the Ala175Glu mutation. Mutagenesis of several flanking residues in PHYL including Arg115, Val117 and Arg125 results in substantial reduction in binding[13]. Moreover, the PHYL (108-130) peptide has previously been shown to bind to Siah with apparent K_D value of 176 nM and competes effectively against many other Siah binding proteins that possess the consensus degron motif[13]. The structure of the Siah:PHYL complex suggests that

arginine residues that flank the consensus sequence might contribute to degron binding in an unspecific manner rather than be critical for the specificity of the substrate recognition, thus explaining the low K_D value of 176 nM of PHYL compared to other targets/peptides. The high affinity binding of PHYL to Siah may represent the adaptor nature of PHYL, whereas the lower affinity of the mammalian interactors may facilitate free transfer from Siah to the proteasome.

The TIEG-1 degradation results support the suggestion that the PHYL/Siah interaction defines a substrate-binding groove on Siah that is utilized by some mammalian proteins. It is not known at this stage whether other proteins are recruited to this complex, or whether Siah itself can facilitate the transfer of ubiquitin from the E2 to the substrate. It is also not known whether both binding grooves within a dimer are utilized, or whether ubiquitin is transferred from an E2 bound to the same Siah monomer as the substrate. Further structural experiments, involving larger protein fragments, will be required to answer these questions.

METHODS

Expression and purification of Siah. Mouse Siah 1a (92-282) was cloned into PMCSG7 and expressed as a His-tag fusion protein in BL21 DE3 Rosetta cells. Protein expression was induced with 0.1 mM IPTG for 3 hours at room temperature when the cell density reached an OD_{600} of 0.6. Siah was purified on a HisTrap (Invitrogen) column. The His-tag was cleaved over 48 hours with a His-tagged TEV protease. TEV, the cleaved His-tag and any uncleaved material were removed by a second round of purification on a HisTrap column. Siah was

further purified by Q-Hyper-D anion exchange in a 0 to 400 mM NaCl gradient at pH 8.0. Prior to crystallization, the protein was desalted on a NAP-25 column using a buffer consisting of 25 mM Tris pH 8.0, 0.2 mM DTT and concentrated using an Amicon concentrator to 10 mg/ml.

Crystallization of Siah-PHYL complex. Siah was mixed with a synthetic Phyllopod (PHYL) peptide 107-130 (Auspep, synthesized with free amino terminus and C-terminal amide, at >95% purity) at a 1:1 ratio and then incubated for 2 hours at room temperature. Crystallization was performed at 295 K using the hanging-drop vapor-diffusion technique. Very thin plate shaped crystals (2 mm x 2 mm x 0.03 mm) grew within a week when 2 µl Siah:PHYL (107-130) was mixed with an equal volume of reservoir solution containing 100 mM Tris pH 8.0, 5% (v/v) MPD, 10 mM Tris(2-carboxyethyl)phosphine hydrochloride (TCEP) and 1.3-1.6 M $MgSO_4$. The presence of PHYL peptide in the crystals was confirmed by resolving dissolved crystals on SDS-PAGE.

Structure determination of Siah1a-PHYL (107-130) complex. Diffraction data were collected at 100 K and recorded on a MAR CCD-165 detector on BioCARS beam line 14-ID-B at the Advanced Photon Source (Chicago, USA). The wavelength was set to 1.117 Å. 10% (v/v) glycerol was used as a cryo-protectant. Data were processed using the HKL package[15]. The diffraction data statistics are shown in Table 1. The structure was determined by molecular replacement. The search model was the Siah-SBD dimer (PDB id: 1K2F) excluding the zinc fingers. Calculations were performed using program Molrep[16] and all data to 4 Å resolution included in the calculations. Two solutions were found that gave a R-factor of 52.1 % and correlation coefficient of 0.46. The solutions were in agreement with the self-rotation

function. Two dimers (including zinc fingers) packed well in the asymmetric unit without any major clashes. The N-terminal zinc finger domains required significant rebuilding. After 4 cycles of refinement and model rebuilding, the density corresponding to PHYL peptide could be unambiguously interpreted anchored at Met 119. The density for 114-124 of PHYL peptide is well determined in all 4 monomers of the Siah molecule that are observed in the asymmetric unit. The final model includes 4 Siah monomers 92-282 including 4 zinc ions and 4 PHYL peptides (114-124). The stereochemical quality of the final model is good (Table 1) with 77.6% residues in the most favored region of the Ramachandran plot, only 3 residues in the generously allowed regions and none in the disallowed regions. Other stereochemical parameters such as side chain chi angle values, peptide bond planarity, alpha-carbon tetrahedral distortions and non-bonded interactions are all better than or within the allowed ranges defined by PROCHECK[17].

Mutagenesis experiments. Siah and TIEG-1 mutants were made using the Stratagene QuikChange Mutagenesis Kit. The mutations were confirmed by restriction enzyme digest and DNA sequencing. The Siah mutants were expressed using the protocol for wild-type Siah and purified using His-Bind Quick 300 Cartridges (Novagen). The His-tag was retained for use in pull-down assays. The mutagenic oligo pairs for Siah are as follows:

GCTGTCGACTGGGTGAAAATGCAGTCTTGTTTTGGC	M180K forward
GCCAAAACAAGACTGCATTTTCACCCAGTCGACAGC	M180K reverse
TCCATTACCACCGACCAAGGAGAAGATATCGTTTTCC	L158D forward
GGAAAACGATATCTTCTCCTTGGTCGGTGGTAATGGAC	L158D reverse
GTCCATTACCACCAAGCAAGGAGAAGATATCGTTTTCC	L158K forward
GGAAAACGATATCTTCTCCTTGCTTGGTGGTAATGGAC	L158K reverse
GGAGAAGATATCGTTTTCAAAGCTACAGACATTAACC	L166K forward

GGTTAATGTCTGTAGCTTTGAAAACGATATCTTCTCC	L166K reverse
CAAGTCCATTGAAACCGACCAAGGAGAAGATATCGTTTTCCTTGC	T156E/L158D forward
GGAAAACGATATCTTCTCCTTGGTCGGTTTCAATGGACTTGTG	T156E/L158D reverse
GAAGATATCGTTTTCAAAGCTCGTGACATTAACCTTCCTGGTGC	L166K/T168R forward
GGAAGGTTAATGTCACGAGCTTTGAAAACGATATCTTCTCCTTGC	L166K/T168R reverse
GATATAGTTTTCCTTGCTCGAGACATTAACCTTCC	T168R forward
GGAAGGTTAATGTCTCGAGCAAGGAAAACTATATC	T168R reverse
CATTAACCTGCCTGGTGAAGTTGACTGGGTGATGATGC	A175E forward
GCATCATCACCCAGTCAACTTCACCAGGCAGGTTAATG	A175E reverse

The mutagenic oligo pair for TIEG-1 were:

CATACCATGTGCCGCTAACTCAAACAACAGATCCAAATGTG	VxP to NxN forward
CACATTTGGATCTGTTGTTTGAGTTAGCGGCACATGGTATG	VxP to NxN reverse

Pull-down assays. 50 µl of Ni-NTA agarose resin (Qiagen) was used for each sample. Siah WT or Siah mutants (approximately 0.04 mM) were mixed with PHYL(107-130) peptide (0.1 mM) in the binding buffer (25 mM Tris pH 8.0, 0.2 M NaCl, 2mM TCEP, 0.1 % Np-40). 6His-galectin-3 + PHYL(107-130), Siah WT with no PHYL(107-130), and PHYL(107-130) alone were used as controls. The samples were pre-mixed and incubated for 20-30 minutes at room temperature. 50 µl Ni-NTA resin was washed 3 times with the binding buffer prior to addition of the samples. The samples were added to the resin and incubated for 40 minutes at room temperature with gentle rocking. The resins were then spun down for 2 min. at 2000 rpm. The supernatants were removed and kept for examination by gel electrophoresis. The resins were washed 3 times with binding buffer and then resuspended in 40 µl of SDS sample buffer and analyzed on a 16.5% Tricine gel. The amount of PHYL bound to Siah was quantitated by scanning

densitometry (Molecular Dynamics) using ImageQuaNT 5.0 software. The measurements were normalized to Siah loading.

Degradation experiments. Transfections were performed in 12-well tissue culture plates using HEK293T cells and Lipofectamine 2000 (Invitrogen) according to the manufacturer's instructions. DNA for Flag-TIEG-1 (in pCDNA4/TO), and HA-Siah1a (pCDNA3) were added as shown in the Figure legend. After 20-24 hours in culture, cells were washed once in 1 ml of PBS, harvested in SDS sample buffer, prior to SDS-PAGE and Western blotting. Blots were probed with anti-Flag antibody (Sigma) for TIEG-1, anti-HA antibody for Siah and PHYL expression, and anti-α-tubulin as a loading control. Expression vector for Flag-TIEG-1 was a gift from Steven Johnsen and Thomas Spelsburg (Mayo Clinic and Foundation, Rochester, NY).

Accession codes. Atomic coordinates and structure factors have been deposited in the Protein Data Bank (accession code 2AN6).

ACKNOWLEDGEMENTS

We thank Harry Tong and other staff at BioCARS for their help with data collection during our visit to the Advanced Photon Source. Access to BioCARS Sector 14 at the Advanced Photon Source at Argonne, Illinois, was provided by the Australian Synchrotron Research Program, which is funded by the Commonwealth of Australia as a Major National Research Facility. BioCARS Sector 14 is supported by the U.S. National Institutes of Health, National Center for Research Resources. The Advanced Photon Source is supported by the U.S. Department of Energy, Basic Energy Sciences, Office of Energy Research. This work was supported by a project grant from the National Health and Medical Research Council of Australia (NHMRC). M.W.P. is a NHMRC Senior Principal Research Fellow and G.P. is supported by a NHMRC RD Wright Research Fellowship.

COMPETING INTERESTS STATEMENT

The authors declare that they have no competing financial interests.

Table 1 Data collection and refinement statistics

	siah_phyl_28
Data collection	
Space group	$P2_1$
Cell dimensions	
a, *b*, *c* (Å)	63.3, 100.0, 103.4
α, β, γ (°)	90.0, 104.3, 90.0
Resolution (Å)	3.0 (3.1-3.0)
R_{merge}	8.2 (50.8)
$I / \sigma I$	13.0 (1.3)
Completeness (%)	99.2 (95.8)
Redundancy	3.2 (3.0)
Refinement	
Resolution (Å)	3.0
No. reflections	23606
R_{work} / R_{free}	23.7 / 30.2
No. atoms	6376
Protein	6024
PHYL peptide/Zn ions	344/8
B-factors	
Protein	75.0
Protein (Siah SBD only)	65.7
Protein (Zn finger domains only)	93.2
PHYL peptide/Zn ions	71.4/96.8
R.m.s. deviations	
Bond lengths (Å)	0.017
Bond angles (°)	1.8

FIGURE LEGENDS

Figure 1 Structure of the Siah (92-282)-PHYL (107-130) complex. (**a**) Orthogonal views of the two dimers observed in the asymmetric unit in ribbon style with the PHYL peptide shown in stick fashion. Substrate binding domains are shown in green and yellow, the first and second zinc finger domains are in red and blue respectively. Zinc ions are denoted as purple spheres. An omitted $F_o - F_c$ electron density map, calculated from the final model after the PHYL peptide was excluded and contoured at 3σ, is shown in light blue. This figure was prepared with Bobscript[18] and rendered with RASTER3D[19]. (**b,c**) Stereo views showing the key interactions between the PHYL peptide (residues underlined) and Siah. Hydrogen bonds are shown as purple dashed lines. The brown dash loop represents the conformation of 172-177 loop observed in the uncomplexed Siah structure. Residues of β1 and β2 of Siah are shown as bonds in (**b**). The hydrophobic pocket of Siah (including residues of strand β0) that harbours PHYL residues Ala118 and Val120 is shown as bonds in (**c**).

Figure 2 Binding groove mutants of Siah fail to bind PHYL. 16.5% tricine gel demonstrating the effect of Siah mutants on PHYL binding as examined in the pull-down assays described in Methods. Bars below the gel represent quantitated amounts of PHYL peptide bound to Siah and mutants.

Figure 3 TIEG-1 degradation is dependent on the PHYL-binding groove of Siah. (**a**) HEK293T cells, in 12-well plates were transfected with 500 ng of Flag-TIEG-1 and 100 ng of HA-Siah1a DNA, expressing wild type and various mutations of residues in the

PHYL-binding groove as described in the Methods. (**b**) TIEG-1 degradation is proteasome-dependent. HEK293T cells were transfected with 500 ng of Flag-TIEG-1, plus and minus 25 ng of HA-Siah1a, in the presence and absence of MG132. (**c**) TIEG-1 degradation is dependent on the VxP Siah-binding motif. HEK293T cells were transfected with 500 ng of Flag-TIEG-1 or Flag-TIEG-1 (VxP to NxN), and 6.25 – 100 ng of HA-Siah1a. TIEG-1 levels were monitored by Western blot probing with anti-Flag antibody. Due to degradation, Siah1a immunoreactivity was not detected reproducibly at or below 100 ng of DNA transfected.

References

1. Ciechanover, A. The ubiquitin-proteasome pathway: on protein death and cell life. *EMBO J* **17**, 7151-7160 (1998).

2. Tang, A.H., Neufeld, T.P., Kwan, E. & Rubin, G.M. PHYL acts to down-regulate TTK88, a transcriptional repressor of neuronal cell fates, by a SINA-dependent mechanism. *Cell* **90**, 459-467 (1997).

3. Li, S., Li, Y., Carthew, R.W. & Lai, Z.C. Photoreceptor cell differentiation requires regulated proteolysis of the transcriptional repressor Tramtrack. *Cell* **90**, 469-478 (1997).

4. Dong, X. *et al.* ebi regulates epidermal growth factor receptor signaling pathways in Drosophila. *Genes Dev* **13**, 954-965 (1999).

5. Boulton, S.J., Brook, A., Staehling-Hampton, K., Heitzler, P. & Dyson, N. A role for ebi in neuronal cell cycle control. *EMBO J* **19**, 5376-5386 (2000).

6. Matsuzawa, S. & Reed, J.C. Siah-1, SIP, and Ebi collaborate in a novel pathway for beta-catenin degradation linked to p53 responses. *Molecular Cell* **7**, 915-926 (2001).

7. Conaway, R.C., Brower, C.S. & Conaway, J.W. Emerging roles of ubiquitin in transcription regulation. *Science* **296**, 1254-1258.

8. Nakayama, K. *et al*. Siah2 regulates the stability of prolyl-hydroxylases, controls HIFa abundance and modulates physiological responses to hypoxia. *Cell* **117**, 941-952 (2004).

9. Liani, E. *et al*. Ubiquitylation of synphilin-1 and α-synuclein by SIAH and its presence in cellular inclusions and Lewy bodies imply a role in Parkinson's disease. *Proc. Natl. Acad. USA* **101**, 5500-5505 (2004).

10. Polekhina, G. *et al.* Saih ubiquitin ligase is structurally related to TRAF and modulates TNF-α signaling. *Nature Struct. Biol*. **9**, 68-75 (2002).

11. Reed, J.C. & Ely, K.R. Degrading liaisons: Siah structure revealed. *Nature Struct. Biol*. **9**, 8-10 (2002).

12. Matsuzawa, S., Li, C., Ni, C.Z., Takayama, S., Reed, J.C. & Ely, K.R. Structural analysis of Siah1 and its interactions with SIP. *J. Biol. Chem*. **278**, 1837-1840 (2003).

13. House, C.M. *et al.* A binding motif for Siah ubiquitin ligase. *Proc. Natl. Acad. Sci.* **100**, 31-1-3106 (2003).

14. Johnsen, S.A., Subramanian, M., Monroe, D.G., Janknecht, R. & Spelsberg, T.C. Modulation of transforming growth factor beta (TGFbeta)/Smad transcriptional responses through targeted degradation of TGFbeta-inducible early gene-1 by human seven in absentia homologue. *J. Biol. Chem*. **277**, 30754-30759 (2002).

15. Otwinowski, K. & Minor, W. Processing of X-ray diffraction data collected in the oscillation mode. *Methods Enzymol.* **276**, 307 - 326 (1997).

16. Collaborative Computational Project Number 4. *Acta Crystallogr. D* **50**, 760-763 (1994).

17. Laskowski, R.A., MacArthur, M.W., Moss, D.S. and Thornton, J.M. PROCHECK: a program to check the stereochemical quality of protein structures. *J. Appl. Crystallogr.* **26**, 283-291 (1993).

18. Esnouf, R. M. Further additions to MolScript version 1.4, including reading and contouring of electron-density maps. *Acta Crystallogr. D* **55**, 938-940 (1999).

19. Merritt, E. A., and Murphy, M. E. Raster3D Version 2.0. A program for photorealistic molecular graphics. *Acta Crystallogr. D* **50**, 869-873 (1994).

.

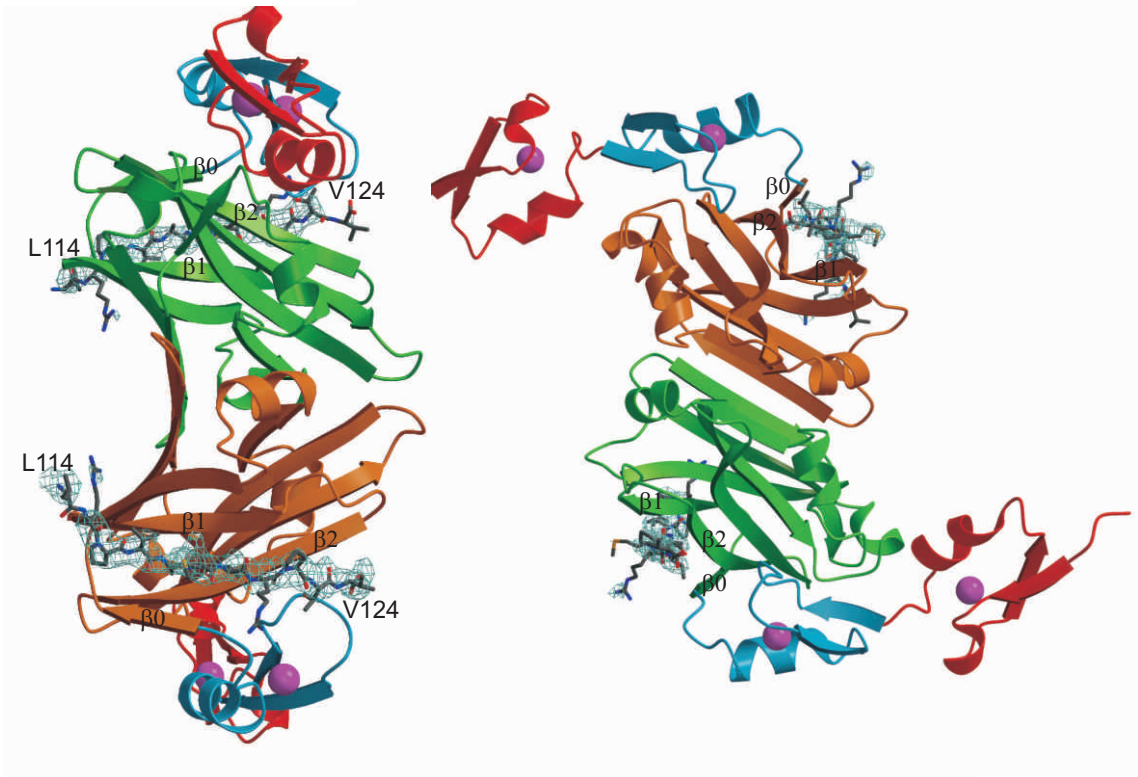
A
β0
V124
β2
L114
β1
L114
β1
β2
V124
β0
β0
β1
β2
β0

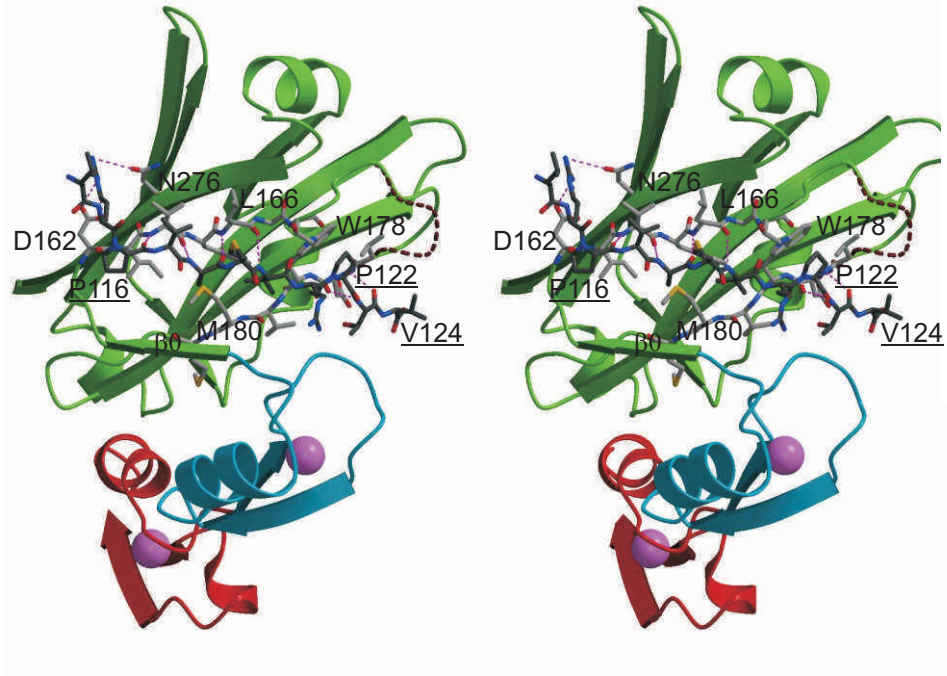
B
N276
L166
D162
W178
P116
P122
M180
V124
β0
N276
L166
D162
W178
P116
P122
M180
V124
β0

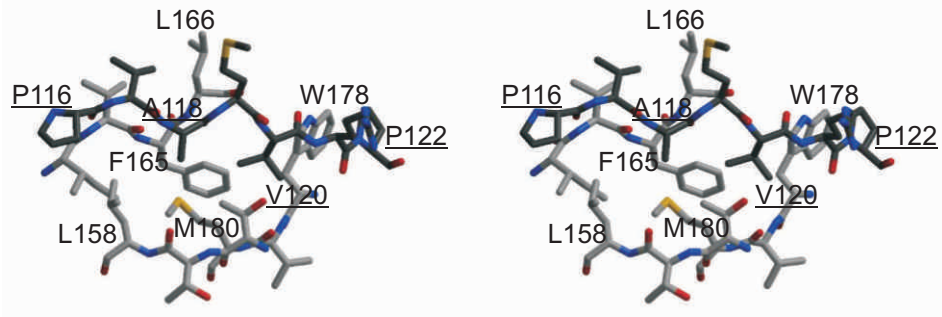
C
L166
P116
A118
W178
P122
F165
V120
L158
M180
L166
P116
A118
W178
P122
F165
V120
L158
M180

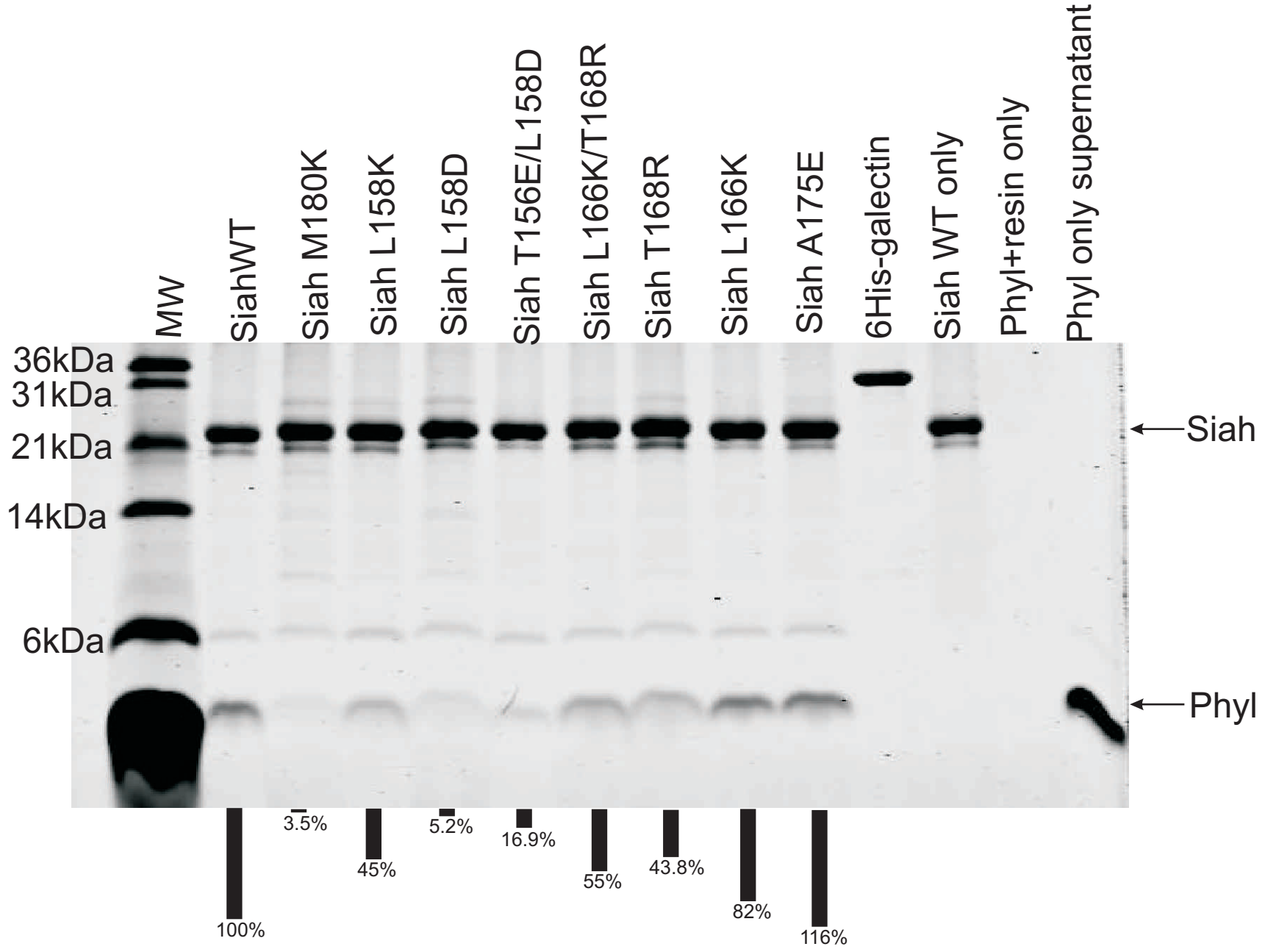
MW
SiahWT
Siah M180K
Siah L158K
Siah L158D
Siah T156E/L158D
Siah L166K/T168R
Siah T168R
Siah L166K
Siah A175E
6His-galectin
Siah WT only
Phyl+resin only
Phyl only supernatant
36kDa
31kDa
21kDa
14kDa
6kDa
Siah
Phyl
100%
3.5%
45%
5.2%
16.9%
55%
43.8%
82%
116%

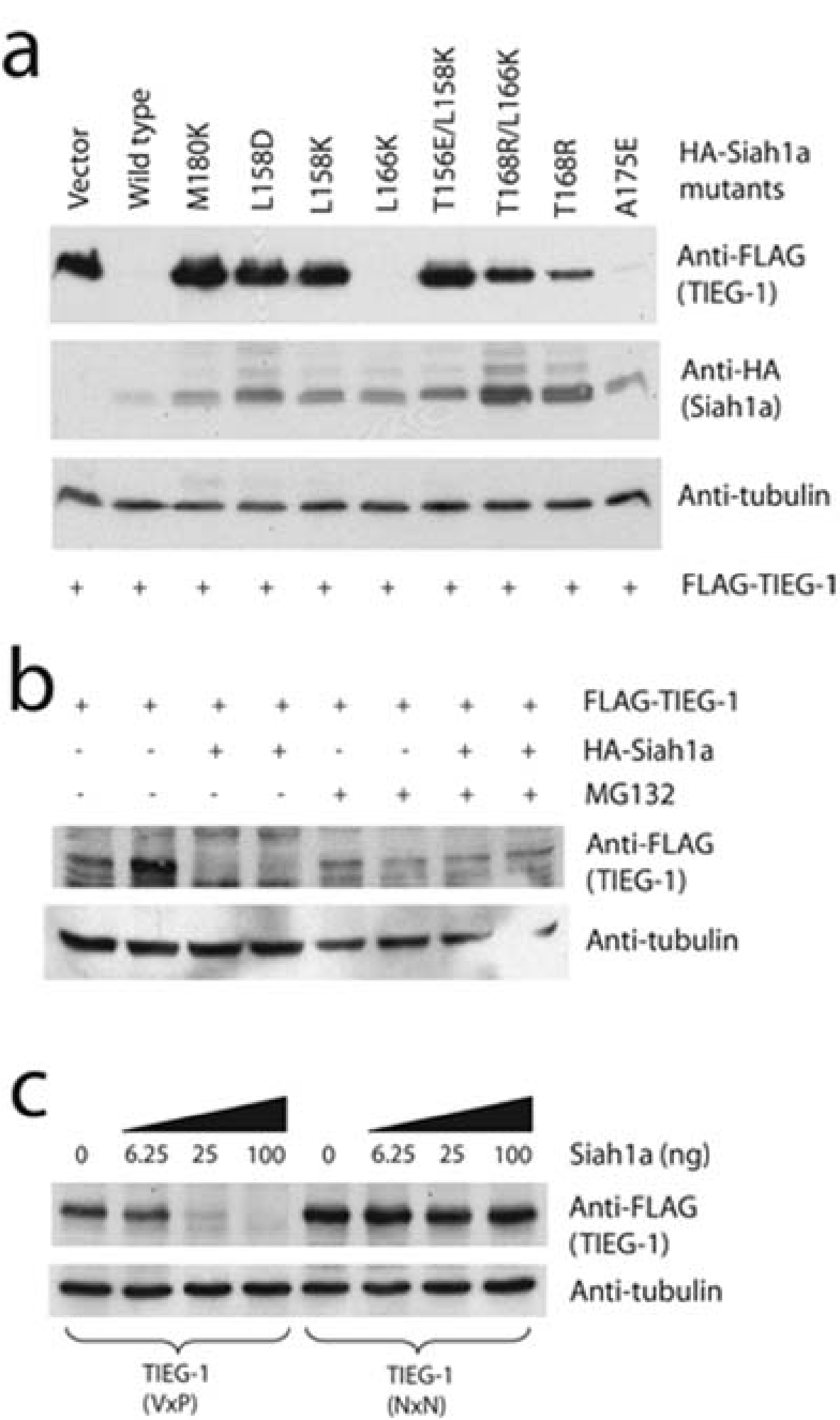
a
Vector
Wild type
M180K
L158D
L158K
L166K
T156E/L158K
T168R/L166K
T168R
A175E
HA-Siah1a mutants
Anti-FLAG (TIEG-1)
Anti-HA (Siah1a)
Anti-tubulin
+ + + + + + + + + +
FLAG-TIEG-1
b
+ + + + + + + +
FLAG-TIEG-1
- - + + - - + +
HA-Siah1a
- - - - + + + +
MG132
Anti-FLAG (TIEG-1)
Anti-tubulin
c
0 6.25 25 100 0 6.25 25 100
Siah1a (ng)
Anti-FLAG (TIEG-1)
Anti-tubulin
TIEG-1 (VxP)
TIEG-1 (NxN)